Electromagnetic Propagation Path and Signal Attenuation Prediction Based on DEM Electronic Map

Ziqi Sun[1], Shengliang Fang[2], Weichao Yang[3], Gongliang Liu[1], and Ruofei Ma[1(✉)]

[1] Harbin Institute of Technology, Weihai 264200, Shandong, China
maruofei@hit.edu.cn
[2] School of Space Information, Space Engineering University, Beijing 101416, China
[3] China Academy of Space Technology (Xi'an), Xi'an 710100, Shanxi, China

Abstract. With the development of information technology, the advantages of information warfare have become increasingly obvious. Wireless communication is the main means of communication in modern warfare. In military wireless communication where the electromagnetic environment of the battlefield is quite complex, the problem of electromagnetic prediction is particularly prominent. Based on the multi-domain grid of the battlefield environment with the help of Digital Geographic Elevation Model (DEM) data, combined with the accurate wireless propagation model, it can make predictions more accurately, and provide data support for wireless network coverage prediction and the discovery of communication blind spots. The main research is the ITU.RP-526 accurate prediction model, which divides obstacles into knife-edge type and round type, and calculates the total propagation attenuation of the path based on the modified free-space attenuation prediction formula. By comparing with Okumura model and Egli, COST model which considers terrain correction factor, it is verified that the calculation accuracy of this design algorithm is high and the result is reasonable. Complete point-to-point radio wave prediction and field strength coverage.

Keywords: Electromagnetic Prediction · DEM · ITU.RP-526 · Propagation Attenuation

1 Introduction

In military communications, both the transmitting antenna and the receiving antenna have the characteristics of movement, and the height of the receiving antenna is often extremely low, and the propagation of radio waves will often be constantly affected by terrain obstacles, buildings and surface vegetation. Applying the traditional artificial field strength prediction method to obtain the field strength prediction map as the basis for network design, not only the workload is large, the efficiency is low, and the results are somewhat random. Therefore, it is necessary to use Digital Elevation Model (DEM) data to obtain geographic information with a certain accuracy, and then through the analysis

A. Li et al. (Eds.): 6GN 2022, LNICST 504, pp. 38–51, 2023.
https://doi.org/10.1007/978-3-031-36011-4_4

of application scenarios and actual conditions, compare various existing radio wave propagation models. Prediction under the premise of good, this can further improve the efficiency of field strength prediction. Compared with traditional paper maps, electronic maps have the advantages of fast storage and display, realization of animations, and the ability to modify and supplement topographic and landform information at any time. With the informatization of wars, military digital maps will play an important role. Therefore, it is of great significance to study the electromagnetic attenuation prediction based on the electronic map under special terrain.

At present, the prediction of electromagnetic radiation is mainly based on ray tracing technology in indoor or urban research. The ray tracing method has become an important tool for propagation prediction due to its high precision [1–5]. The algorithm is mainly divided into four modules, namely the ray-plane intersection calculation module, ray information module, calculation module and ray path tracing module. The four modules can call each other. The ray path tracing module will return all qualified ray path information. Literature [6] proposed grid-based electromagnetic prediction of urban environment, using distributed grid computing to reduce the workload and speed up the calculation, but it did not reflect the accuracy and reliability of the prediction.

There have been many achievements in the research of radio wave propagation theory, and many radio wave propagation models have been established. Divided by research methods, including empirical model, deterministic model and semi-empirical semi-deterministic model. The empirical model is a formula summed up by a large amount of measurement data after statistical analysis. Typical examples include the Egli model, the Okumura-Hata model, the CCIR model, and the COST 231-Hata model. The empirical model does not require detailed environmental information, and can only adapt to the field strength prediction of a specific environment, and the prediction results have large errors. Semi-empirical and semi-deterministic models require environmental information to obtain predicted values. When the environment is not too complex, the prediction accuracy is higher, such as the Longley-Rice model. The deterministic models are all based on electromagnetic wave theory and do not rely on measurement results. Instead, a large number of terrain and architectural details are required for accurate electromagnetic wave path loss prediction and field strength distribution. Typical examples are: ITU-R P.368, ITU-R P.526, ITU-R P.452, Durkin model, Johnson-Gierhart model, etc.

2 Electromagnetic Diffraction Theory

2.1 ITU.RP-526 Model Algorithm

In free space, the propagation of electromagnetic waves is a relatively simple natural phenomenon, but due to the diversity of the surface environment, the prediction of the propagation of electromagnetic waves on the surface is a relatively complicated process. Electromagnetic waves also have different propagation processes in different ground environments, and exhibit different propagation mechanisms such as reflection, refraction, diffraction, transmission and scattering [7]. The main channel of radio wave propagation is an ellipsoid with the transmitting and receiving antenna as the focal point, that is, the first Fresnel zone in space. In this paper, the ITU-R. P 526 model and

the field strength prediction algorithm in the presence of side obstacles jointly predict the field strength attenuation under special terrain. The algorithm of the ITU-RP.526 model mainly includes ground type analysis, line-of-sight determination, obstacle type determination, obstacle number calculation, and loss calculation for various scenarios, as shown in Fig. 1.

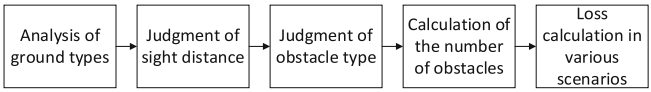

Fig. 1. Algorithm flow chart of the model ITU.RP-526

2.2 Attenuation Calculation Applied to Different Scenarios

The calculation method for different scenarios is more complicated. For details, please refer to Recommendation ITU-RP.526-11 issued by the International Telecommunication Union [7].

Diffraction Within A Smooth Spherical Line-of-Sight Range
The transmission loss is

$$L(\mathrm{X}) = \begin{cases} 11 + \log(X) - 17.6X \\ -20\log(X) - 5.6488X^{1.425} \end{cases} \tag{1}$$

Among them, X is the distance of the path between the transmitting and receiving antennas.

Diffraction Within The Horizon of a Smooth Spherical Surface
Find the minimum distance between the transmitting and receiving antenna line and the surface of the earth, as shown in Fig. 2:

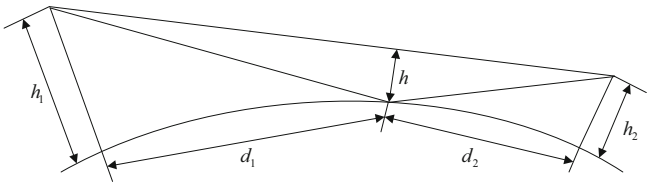

Fig. 2. Schematic diagram of the minimum point of transmission clearance

The calculation formula of the minimum distance h is:

$$h = \frac{\left(h_1 - \frac{d_1}{2a_e}\right)d_2 + \left(h_2 - \frac{d_2}{2a_e}\right)d_1}{d} \tag{2}$$

The threshold distance h_{req} of diffraction loss is:

$$h_{req} = 0.552\sqrt{\frac{d_1 d_2 \lambda}{d}} \tag{3}$$

If $h \geq h_{req}$, it means that the diffraction loss of transmission is zero, and the diffraction calculation ends, otherwise the following operations continue. The calculation of the attenuation L_{req} of the diffracted transmission at the smooth earth horizon is:

$$L = (1 - h/h_{req})L_{req} \tag{4}$$

Diffraction of Independent Peak-Shaped Obstacles
The ideal scenario is shown in Fig. 3:

$$v = 0.0816h\left[\frac{f(d_1 + d_2)}{d_1 d_2}\right] \tag{5}$$

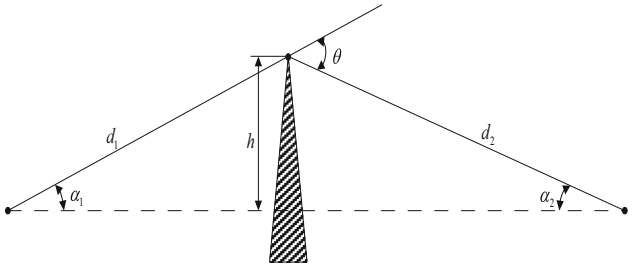

Fig. 3. Ideal spike-shaped obstacle diagram

In the formula, v is the normalized geometric parameter used to mark obstacles; h is the Fresnel clearance, which may be a negative value, in m; f is the signal frequency in MHz; d_1 and d_2 are the path length, in units km.

The mathematical relationship between the diffraction attenuation $J(v)$ and v is:

$$J(v) = -20\log\left(\frac{\sqrt{[1 - C(v) - S(v)]^2 + [C(v) + S(v)]^2}}{2}\right) \tag{6}$$

The following formulas are often used in actual calculations:

$$J(v) = \begin{cases} 6.9 + 20\log\left(\sqrt{(v - 0.1)^2 + 1} + v + 0.1\right) & v > -0.78 \\ 0 & v \leq -0.78 \end{cases} \tag{7}$$

Diffraction of Two Consecutive Peak-Shaped Obstacles
The ideal scenario is shown in Fig. 4:

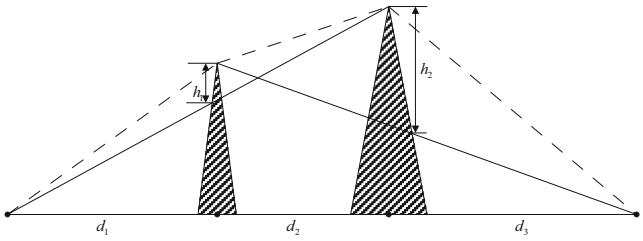

Fig. 4. Two consecutive spike-shaped obstacles

For the diffraction of two peak-shaped obstacles, it can be calculated by splitting into two independent peak-shaped obstacles. The diffraction attenuation generated by the two obstacles is superimposed, and finally the correction item can be used to correct it. Then, the key to this scenario calculation is whether the correction term is accurate.

Two consecutive peak obstacles are divided into two situations, one is that the two obstacles are basically the same, and the other is that the obstacles have obvious primary and secondary differences. When the two peak-shaped obstacles are basically the same, the formula for the correction term:

$$T_c = 10\log\left[\frac{(d_1+d_2)(d_2+d_3)}{d_2(d_1+d_2+d_3)}\right] \tag{8}$$

When two peak-shaped obstacles have obvious primary and secondary differences, the correction term calculation formula:

$$T_c = \left[12 - 20\log_{10}\left(\frac{2}{1-\alpha/\pi}\right)\right]\left(\frac{q}{p}\right)^{2p} \tag{9}$$

$$p = \left[\frac{2(d_1+d_2+d_3)}{\lambda d_1(d_2+d_3)}\right]^{\frac{1}{2}} h_1 \tag{10}$$

$$\tan\alpha = \left[\frac{d_2(d_1+d_2+d_3)}{d_1 d_3}\right] \tag{11}$$

The total diffraction loss is:

$$L = L_1 + L_2 - T_c \tag{12}$$

Diffraction of Cascading Spike-Shaped Obstacles

Represents the scene that occurs when the signal transmission path passes through multiple spike-shaped obstacles connected together. The calculation method of diffraction in this scenario is somewhat similar to that of the double peak. First, find the main peak of diffraction, that is, find the maximum point n of the geometric parameter v, and calculate the diffraction loss $J(v_n)$ according to the method of single-peak diffraction. At that time, the diffraction losses $J(v_{tn})$ and $J(v_{nr})$ between the transmitter and n points

and between n points and the receiver were calculated respectively. The mathematical expression is:

$$L = \begin{cases} J(v_n) + T[J(v_{nr}) + J(v_{tn}) + C] & v_n > -0.78 \\ 0 & v_n \leq -0.78 \end{cases} \tag{13}$$

Diffraction of a Single Circular Obstacle

The circular obstacle is different from the blade shape. The geometric shape of the obstacle is similar to that of a semicircle. The ideal scene is as follows (Fig. 5):

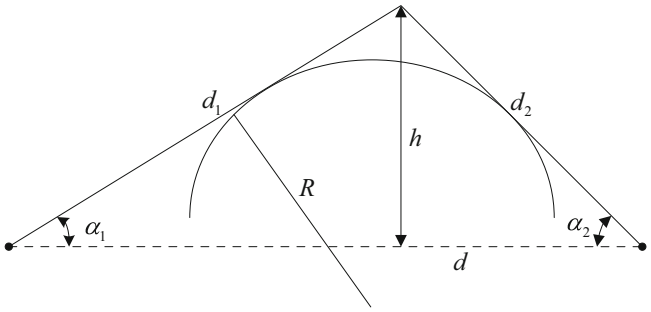

Fig. 5. Schematic diagram of an ideal cylindrical obstacle

The diffraction loss in this scenario is:

$$L = J(v) + T(m, n) \tag{14}$$

In the formula, $J(v)$ is the attenuation caused by the equivalent peak-shaped obstacle at the apex, and $T(m,n)$ is the attenuation related to the curvature of the occlusion.

$$T(m, n) = \begin{cases} 7.2m^{1/2} - (2 - 12.5n)m + 3.6m^{3/2} - 0.8m^2 & mn \leq 4 \\ -6 - 20\log(mn) + 7.2m^{1/2} - (2 - 17n)m + 3.6m^{3/2} - 0.8m^2 & mn > 4 \end{cases} \tag{15}$$

$$m = R\left[\frac{d_1 + d_2}{d_1 d_2}\right] \Big/ \left[\frac{\pi R}{\lambda}\right]^{1/3} \tag{16}$$

$$n = h\left[\frac{\pi R}{\lambda}\right]^{2/3} \Big/ R \tag{17}$$

2.3 Attenuation Prediction of Electromagnetic Propagation

The attenuation prediction of electromagnetic propagation mainly considers line-of-sight propagation, diffraction propagation, tropospheric scattering propagation, atmospheric

Table 1. Calculation of total attenuation in different scenarios

Path type	Calculation formula
Line-of-sight propagation path	$L_b(p) = L_{b0}(p) + A_{ht} + A_{hr}$
Diffraction propagation path	$L_b(p) = L_{b0}(p) + L_{ds}(p) + A_{ht} + A_{hr}$
Tropospheric scattering path	$L_b(p) = -5\log\left(10^{-0.2L_{bs}} + 10^{-0.2L_{bd}} + 10^{-0.2L_{bam}}\right) + A_{ht} + A_{hr}$

reflection, additional scattering loss, etc. The specific attenuation calculations are shown in Table 1.

$L_{ds}(p)$ is the predicted transmission loss of time p% given by the partial diffraction path of the diffraction propagation model. L_{bs} is the basic transmission attenuation caused by the tropospheric scattering model. L_{bd} is the basic transmission attenuation caused by the diffraction propagation model. L_{bam} is the corrected attenuation caused by atmospheric reflection. All the above attenuation parameters can be calculated from the empirical formulas in the ITU. RP. 526 recommendations.

3 Model Establishment

Digital elevation model (DEM) refers to a collection of geographic elevation data within a certain range to describe the spatial distribution of actual terrain features. Digital elevation model is an important format of electronic map, which has a wide range of applications in the fields of national economy and national defense construction, as well as humanities and natural sciences. The standard definition of a digital elevation model is a combination of three-dimensional vectors representing the attributes of the surface space, represented by (x, y, z), where (x, y) represents the location information, and z represents the elevation information of the location, in discrete points Build a model to describe the continuous topography. In practical applications, DEM is usually expressed as a raster data, but it is different from ordinary image information raster data. An ordinary image pigment point is just a simple discrete point, which only represents the attribute information of the point. There is no topological relationship between points, and DEM elevation data not only express the elevation information of the corresponding point, but also express the elevation information of the area between the points through the topological relationship between the points. The data source of this article is SRTM data, and the accuracy of the data is 3arc-seconds. First, download the SRTM data through the Internet, and then convert it to the required DEM data format through the Global mapper software.

When obtaining the path profile data between the transmitter and the receiver, after determining the position of the transmitter and the receiver, you need to determine the number of points that need to be taken for the entire path according to the accuracy requirements, and adopt the method of sampling at equal intervals, and each sampling point the position of can be calculated. Since the sampling points cannot completely correspond to the geographic elevation data points, elevation interpolation is required

for each sampling point and two endpoints, so as to obtain the elevation data at equal intervals on the entire path, based on which the profile curve can be obtained. There are many interpolation methods, including high-order polynomial interpolation, spline function interpolation, bilinear interpolation, spline function fitting interpolation, polynomial fitting interpolation, moving surface fitting method, and weighted average method. The elevation data in this paper adopts regular grid data, so the bilinear polynomial interpolation method can simplify the calculation and have higher accuracy. The bilinear polynomial interpolation uses the four other known elevation data points that are closest to the unknown elevation point and surrounds it to perform surface fitting. The schematic diagram is shown in Fig. 6. For each sampling point P, four points A, B, C, and D with known elevations around it can be found. Their elevation values are H_a, H_b, H_c, H_d, and the elevation value of point P is:

$$H_p = (1 - dx)(1 - dy)H_c + dx(1 - dy)H_d + dxdyH_b + (1 - dx)dyH_a \tag{18}$$

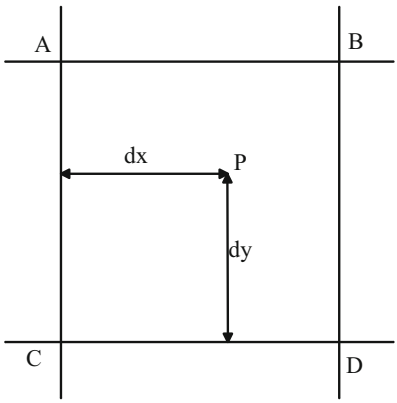

Fig. 6. Schematic diagram of bilinear polynomial interpolation

4 Example of Different Scenario Analysis

The attenuation of electromagnetic signal strength is mainly affected by the signal frequency, distance and obstacles. In this part of the simulation, the signal frequency is fixed to 460 MHz. In practical applications, the radar needs to detect the frequency of the received signal and use the frequency as the input for calculation. The reference points affected by obstacles are mainly ground reference points, and the reference points in the air are regarded as free space propagation loss during simulation, so only the signal vector of the ground reference point is considered when the monitoring stations are deployed later. The test results of the electromagnetic signal attenuation prediction algorithm are as follows. The test is carried out for different terrain conditions, and the simulation results of multiple propagation paths and propagation attenuation are obtained.

The following simulation diagrams show the comparison between the path profiles and the calculation results of the attenuation program under different conditions and a variety of classical wave propagation models. When it is determined that there is no obstacle on the path, as shown in Fig. 7, it is considered to be a smooth earth, and the free space attenuation is calculated, and the running result of the program is close to the classical model.

When it is determined that there is a single spike-shaped obstacle on the path, as shown in Fig. 8, when the electromagnetic signal passes through the obstacle, it can be seen that there is obvious attenuation, and the total attenuation after passing through the obstacle through diffraction is about 20dB higher than that of the classical model. This is consistent with the previous understanding of obstacle diffraction and has higher accuracy.

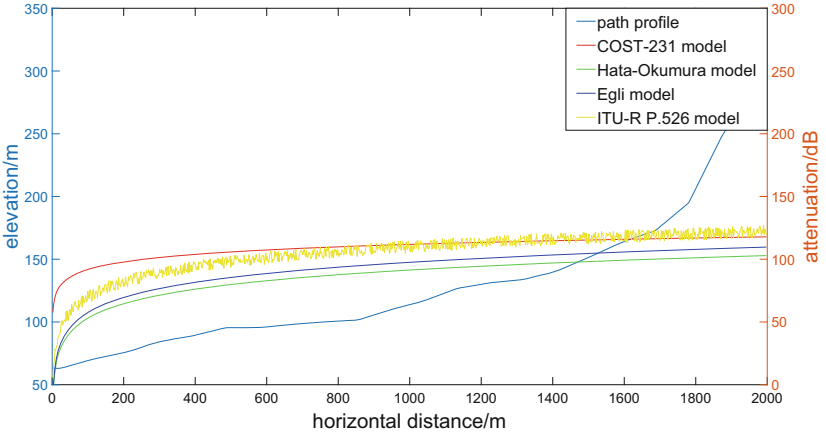

Fig. 7. Attenuation prediction without obstacles

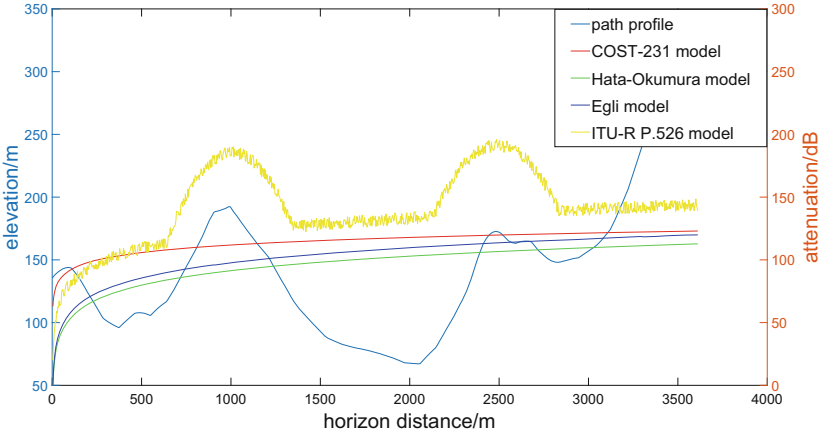

Fig. 8. Attenuation prediction in the case of a single spike-shaped obstacle

When it is determined that there is a single circular obstacle on the path, as shown in Fig. 9, when the electromagnetic signal passes through the obstacle, it can be seen that there is obvious attenuation, but the attenuation is significantly smaller than the diffraction attenuation of the spike-shaped obstacle, and the electromagnetic signal passes through the obstacle. The total attenuation behind the obstacle is close to the classical model. It can be seen that the circular obstacle has little influence on the diffraction attenuation, and the attenuation can be approximately ignored when the width of the obstacle is small compared to the length of the entire path.

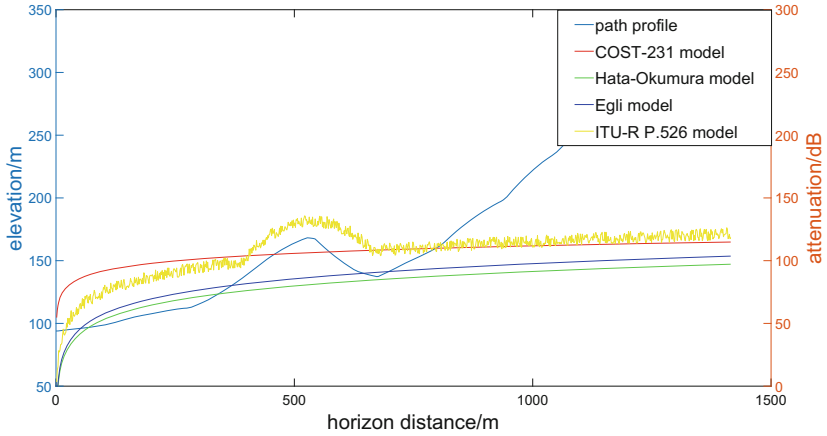

Fig. 9. Attenuation prediction in the case of a single circular obstacle

When it is determined that there are multiple cascading obstacles on the path, as shown in Fig. 10, according to the decomposition principle mentioned above, the previous obstacle vertex is used as the electromagnetic radiation source for the subsequent diffraction calculation, and the multiple levels The connected obstacles are decomposed into multiple separate obstacles for processing. It can also be seen from the figure that the electromagnetic signal undergoes multiple stages of attenuation. After passing through an obstacle, the next diffraction value does not return to the original attenuation value. Calculated, the final total attenuation also superimposes the attenuation value of multiple diffractions, and the gap with the classical model is larger than that of a single obstacle, and the specific increase depends on the number of cascaded obstacles.

Through the simulation test, it can be seen that the electromagnetic prediction program can roughly simulate the propagation path and propagation loss of the electromagnetic radiation signal when it is diffracted by various obstacles on various terrains. Since the propagation path of the electromagnetic signal is predicted and more Factors affecting the propagation and attenuation of electromagnetic signals, the final signal attenuation value calculated by this algorithm is generally higher than the traditional propagation attenuation algorithm, and the signal path and attenuation prediction effect is ideal.

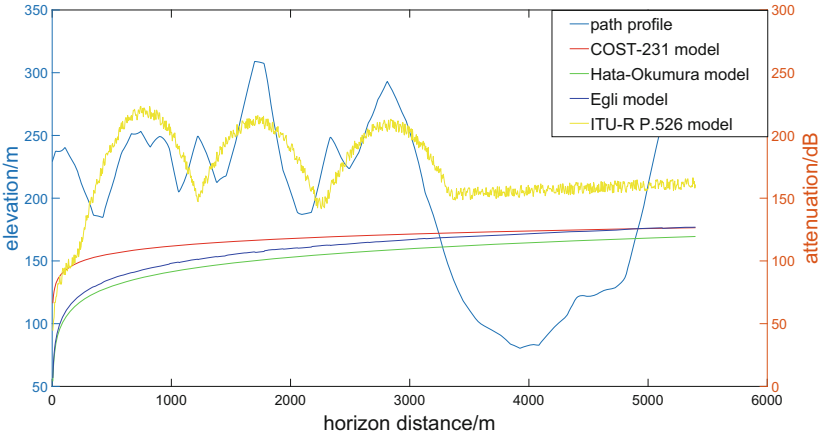

Fig. 10. Attenuation prediction in case of cascading obstacles

Using the elevation data of parts of Shandong, China, set the transmitter positions as E121.0574 and N37.2188, and the receiver positions as E121.7379 and N37.2561, as shown in Fig. 11. Obtain the path profile data according to the above method, and draw the path profile as shown in Fig. 12.

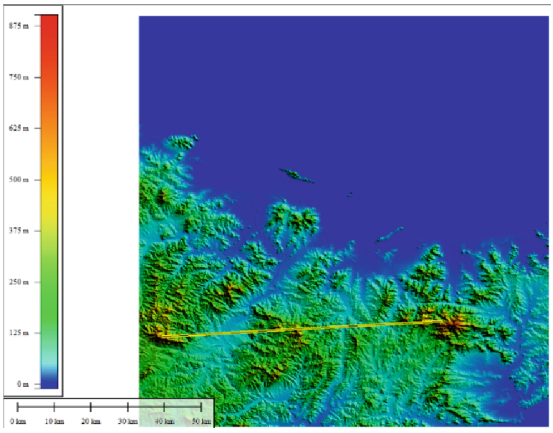

Fig. 11. Determining the position of transmitter and receiver in digital map

The program initialization input parameters are shown in Table 2.

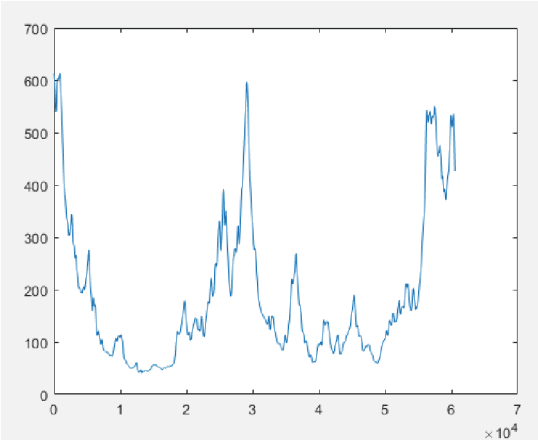

Fig. 12. Electromagnetic radiation path profile

Table 2. Input parameter settings

Enter parameter name	Input parameter value
Percentage of time p_w	50
Mean atmospheric refractive index gradient ΔN	45
Sea level refractive index N_0	325
Signal frequency f(MHz)	460
Transmit antenna height h_t(m)	10
Receiving antenna height h_r(m)	10
Transmit antenna gain G_t(dBW)	30
Receive antenna gain G_r(dBW)	30
Transmitting antenna position	E121.0574, N37.2188
Receiving antenna position	E121.7379, N37.2561

The simulation result of the program is shown in Fig. 13, which includes the topographic profile of the propagation path, the attenuation curve calculated according to the ITU-R P.526 model, and the Okumura-Hata model, Egli model and COST-231 model are set as a comparison. The attenuation value at the receiving antenna calculated according to the ITU-R P.526 model is 201.6587 dB. Because of the diffraction loss and the attenuation in various scenarios, the calculated attenuation value is slightly higher than the attenuation value obtained under the empirical model. Electromagnetic wave propagation is line-of-sight propagation. It can be seen that when obstacles pass through the propagation path, the attenuation value increases significantly. As the distance increases and the height of the receiving point increases, the attenuation value will continue to

decrease to similar to free space propagation, but still The attenuation value will be higher due to the influence of obstacles.

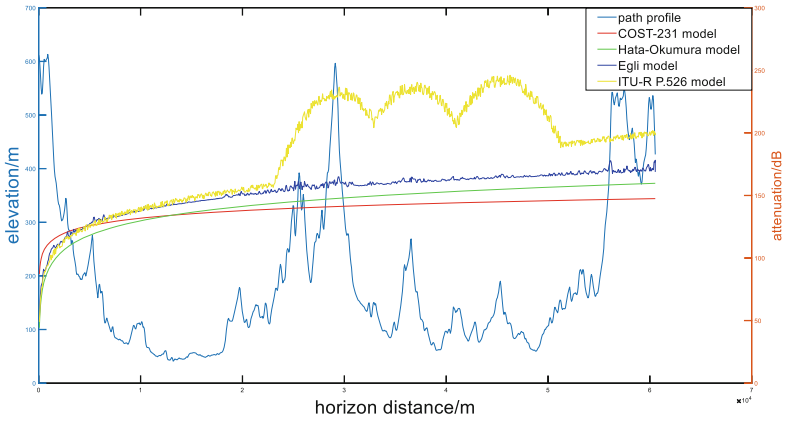

Fig. 13. Simulation result graph

5 Conclusion

Aiming at the complex and changeable terrain of the battlefield, this paper uses digital geographic elevation model data combined with the deterministic model of wireless diffraction propagation to classify and calculate the obstacles in the terrain, predict the electromagnetic environment of the battlefield, and calculate the target position The propagation path and attenuation value at the location. By comparing with Okumura model and Egli, COST model considering the terrain correction factor, it is concluded that the calculated attenuation value is slightly higher than the attenuation value obtained under the empirical model, and the electromagnetic wave propagation is line-of-sight propagation. When passing obstacles on the path, the attenuation value increases significantly. As the distance increases and the height of the receiving point increases, the attenuation value will continue to decrease to similar to free space propagation, but it will still be affected by the obstacles and make the attenuation value higher. Therefore, when the signal is blocked by a mountain, the attenuation value increases sharply, and the electromagnetic wave propagation link should avoid mountain blocking as much as possible. Therefore, when deploying a monitoring station, it should be deployed in a higher altitude area as much as possible. It has been verified that the calculation accuracy of the algorithm in this paper is high and the results are reasonable. It can be applied to the prediction of the electromagnetic environment of the battlefield, which is of great significance to the future electromagnetic spectrum warfare.

References

1. Rizk, K., Wagen, J.-F., Gardiol, F.: Two-dimensional ray-tracing modeling for propagation prediction in microcellular environments. J. IEEE Train. Veh. Technol. **46**, 508–518 (1997)

2. kreuzgruber, P., Unterberger, P., Gahleitner, R.: A ray splitting model for indoor radio propagation associated with complex geomehies. In: Conference Proceedings of the 1993 43rd IEEE Vehicular Technology Conference, pp.227–230. IEEE (1993)
3. McKown, J.W., Hamilton Jr., R.L.: Ray tracing as design tool for radio networks. J. IEEE Network Mag. **S**, 27–30 (1991)
4. Seidel, S., Rappaport, T.: A ray-tracing technique to predict path loss and delay spread inside buildings. Conf. IEEE Globecom **92**, 649–653 (1992)
5. Valenzuela, R.A.: A ray-tracing approach to predicting indoor wireless transmission. In: Conference Proceedings of the 1993 IEEE 43rd Vehicular Technology Conference, Piscataway, NJ, pp. 214–218. IEEE Press (1993)
6. Coco, S., Laudani, A., Pollicino, G.: GRID-based prediction of electromagnetic fields in urban environment. J. IEEE Trans. Magnet. **45**(3) (2009)
7. ITU International Telecommunication Union. Recommendation TU-R P.526–11. http://www.itu.int/pub1/R-REC/en